Global simulation of the GAM oscillation and damping in a drift kinetic model

S. Satake

National Institute for Fusion Science, Toki, Japan

e-mail contact of main author : satake.shinsuke@nifs.ac.jp

Abstract. Collisionless damping of the geodesic acoustic mode (GAM) is investigated by a drift kinetic simulation. The main subject of the study is to analyze how the magnetic configuration and the finite-orbit-width (FOW) effect of the ion drift motion affect the collisionless damping of GAM. We utilize the neoclassical transport code "FORTEC-3D", which solves the drift kinetic equation based on the delta-f method, to study these issues. In recent analytical study on GAM and zonal flow it is found that the FOW effect and the helical components of magnetic field spectrum change the damping rate of the GAM oscillation. We inspect the change of the damping rate in our simulation. First, the dependence of the damping rate on the FOW effect is investigated. We find that the collisionless damping becomes faster as typical banana width becomes wider. On the other hand, the damping rate in helical magnetic configuration is mainly determined by the effect of helical ripples. It is found that the sideband components, which appear as the axis moves inward, make the GAM damping faster. This result suggests the possibility of controlling both the neoclassical transport level and the GAM oscillation, or zonal flow, in helical plasma. The collisional effect on the GAM damping is also investigated in banana and plateau regimes.

1. Introduction

Zonal flow and the GAM oscillation in toroidal plasmas have been investigated intensively in the recent fusion research, as it is expected that the zonal flow suppresses micro instabilities and anomalous transport. Theoretical investigations and simulation studies on these issues have been done in several models. Recently the analysis have been extended for helical configurations by Watari *et al.*[1] based on the drift kinetic model, and also by Sugama and Watanabe[2] based on the gyrokinetic model. They showed that the GAM frequency and damping rate in helical plasmas depend on the magnetic field spectrum. Sugama and Watanabe also suggested that the GAM damping becomes rapider if the finite-orbit-width (FOW) effect of particle drift orbits is considered in gyrokinetic model. Another interest in GAM oscillation is the collisional damping process. A summary of the previous work concerning collisional damping of poloidal rotation can be found in Lebedev's paper[3]. In the present article, we inspect these effects by using a numerical simulation. For this purpose, we adopt the neoclassical transport code FORTEC-3D[4], which solves the drift kinetic equation for ions in five-dimensional phase space. FORTEC-3D properly treats the finite-orbit-width effect and Coulomb collision operator, and can solve drift kinetic equation in general three-dimensional magnetic field configuration. The time evolution of the radial electric field of the whole plasma confined region can be solved at once. In that sense, our study is an extension of the previous research by Novakovskii *et al.*[5] which investigated the GAM damping in tokamak using a drift kinetic equation solver on a single flux surface. Here, we inspect how the FOW effect, three-dimensional magnetic configuration, and collisions affect the GAM oscillation. Usually drift kinetic simulations require less computation resources and are easier to conduct non-local, global simulation compared with gyrokinetic

ones. Therefore it is useful to obtain the knowledge about GAM, though our simulation cannot treat nonlinear saturation of zonal flow, which is one of the main subjects in gyrokinetic study.

The remainder of this paper is organized as follows: In Sec. 2, the simulation model is briefly explained. Expectation on the behavior of GAM from Sugama and Watanabe's theory are also mentioned there. In Sec. 3 to 5, we investigate (i) the finite-orbit-width effect, (ii) the effect of helical magnetic configuration, and (iii) collisional damping of GAM. Section 6 contains the summary and discussion of the result.

2. Simulation model

A magnetic coordinates (ρ, θ, ζ) is used to represent magnetic field, where $\rho = \sqrt{\psi/\psi_a}$ is a radial coordinate and ψ_a is the toroidal flux label on the boundary. To solve the time development of a plasma distribution function in the phase space $(\rho, \theta, \zeta, \mathcal{K} = v^2, \mu = mv_\perp^2/2B)$ the drift kinetic equation for perturbation $\delta f = f - f_M$,

$$\frac{D\delta f}{Dt} \equiv \left[\frac{\partial}{\partial t} + \dot{\mathcal{K}} \frac{\partial}{\partial \mathcal{K}} + (\mathbf{v}_\parallel + \mathbf{v}_d) \cdot \nabla - C_{tp} \right] \delta f = -\mathbf{v}_d \cdot \left(\nabla f_M - \frac{e\mathbf{E}_\rho}{T} \right) f_M + \mathcal{P} f_M \quad (1)$$

is considered. Here, $\mathbf{E}_\rho = -d\Phi/d\rho \nabla\rho$ is radial electric field, $\mathbf{v}_d$ is the drift velocity of a guiding center, and f_M is a local Maxwellian. It is assumed that density, temperature, and electrostatic potential Φ are flux-surface variables. The test-particle collision operator C_{tp} is implemented numerically as a random kick in the velocity space. The field-particle collision operator $\mathcal{P} f_M$ is defined so as to satisfy the conservation lows for particle number, parallel momentum, and energy[6]. Note that the FOW effect is included in the term $\mathbf{v}_d \cdot \nabla \delta f$, which is usually dropped in standard local transport models. We adopted the two-weight scheme[7] Monte-Carlo method to solve Eq. (1). Two weights of the simulation marker w and p which satisfy the relation $wg = \delta f$, $pg = f_M$ are introduced, where g is the distribution function of simulation markers. Each marker follows the track in the phase space according to the lhs of eq. (1), that is, $Dg/Dt = 0$. Then the evolution of weights for each marker is as follows:

$$\dot{w} = \frac{p}{f_M} \left[-\mathbf{v}_d \cdot \left(\nabla - \frac{e\mathbf{E}_\rho}{T} \right) + \mathcal{P} \right] f_M, \quad (2)$$

$$\dot{p} = \frac{p}{f_M} \mathbf{v}_d \cdot \left(\nabla - \frac{e\mathbf{E}_\rho}{T} \right) f_M. \quad (3)$$

Next, self-consistent time evolution of the radial electric field is solved according to

$$\left(\langle |\nabla\rho|^2 \rangle + \left\langle \frac{c^2}{v_A^2} |\nabla\rho|^2 \right\rangle \right) \epsilon_0 \frac{\partial E_\rho(\rho, t)}{\partial t} = -e \left(Z_i \Gamma_i^{neo} - \Gamma_e^{neo} \right), \quad (4)$$

where the ion flux is obtained by taking volume averaged radial flow

$$\Gamma_i^{neo}(\rho) = \left\langle \int d^3\mathbf{v} \dot{\rho} \, \delta f_i \right\rangle_\rho \simeq \frac{1}{\Delta V(\rho)} \sum_{\{j|\mathbf{x}_j \in \Delta V\}} w_j \dot{\rho}_j \quad (5)$$

within a thin layer $\Delta V(\rho)$ which contains the flux surface ρ. In tokamak cases, Γ_e^{neo} is negligible since $|\Gamma_e/\Gamma_i| \sim O(\sqrt{m_e/m_i})$. In non-axisymmetric cases, however, Γ_e^{neo} is comparable to Γ_i^{neo} and the balance between these two fluxes determines the ambipolar E_ρ. Since ion

and electron fluxes are strongly dependent on E_ρ in the low-collisionality regime, we need a proper evaluation for Γ_e as well as Γ_i to evaluate neoclassical flux or to simulate GAM in helical plasma. However, solving both ion and electron transport by δf scheme is not a practical way because the orbit time scales of two species are too separated. Then, only the ion part is solved by using the δf method. The table of $\Gamma_e^{neo}(E_\rho, \rho)$ for a given profile is prepared by GSRAKE[8], which solves the bounce-averaged drift kinetic equation numerically, and the table is referred to at each time step in solving Eq. (4) in FORTEC-3D. Therefore, the FOW effect of electrons and the rapid adiabatic response of electrons along the magnetic field lines are neglected in our model.

Now let us mention briefly about the effect of the helical components of magnetic field and the finite-orbit-width effect suggested from Sugama and Watanabe's gyrokinetic model. In their analytical approach, they retained the 1st-order correction of the FOW effect of passing particle and the effect of helical components of Fourier spectrum of the field $B_{m,n}$ in evaluation the damping rate of oscillating GAM. From the FOW effect, not only the passing particles which satisfy the resonant condition $\omega - v_\parallel/R_0 q = 0$ but also the second harmonics $\omega - 2v_\parallel/R_0 q = 0$ can contribute collisionless Landau damping of GAM. The helical $B_{m,n}$ modulate particle motion along the field line and change the damping rate and the GAM frequency. The FOW effect always enhances the damping rate, but the contribution of helical ripples are more complicated. In a approximated form they derived, the dependency of the damping rate on magnetic field is represented as a function of relative magnitude of each component $B_{m,n}/B_{0,0}$. Our model, in which only the flux-surface averaged potential $\Phi(\rho)$ is considered and the electron motion is neglected, corresponds to the cold-electron limit $T_e/T_i \to 0$ of their model. However, the basic physics of collisionless GAM damping are retained in our drift kinetic model, and our simulation results can be used to expect the behavior of GAM oscillation with these effects considered here.

3. Collisionless GAM damping (i) Finite-orbit-width effect

Here, to investigate the finite-orbit-width effect, we conduct simulations in a simple tokamak geometry. The safety factor is flat $q \simeq 2.5$, and the major and minor radius are $R_0 = 3.5$m and $a = 1.0$m, respectively. Collision terms are artificially dropped in these calculations. The radial excursion of drift orbit is controlled by changing the strength of the magnetic field on the axis $|B_0|$. Figure 1 shows the time evolution of ion neoclassical flux on two flux surfaces with different $|B_0|$. One can see that the GAM damping is rapider as B_0 is smaller, i. e. , as the drift width becomes larger. In Fig. 2, the damping rate is evaluated from the envelope shape of the wave pattern in Fig. 1. Here, we assume a exponential damping $\Gamma_i \sim \Gamma_0 \exp[-(\gamma - iw)t]$. Sugama and Watanabe's analysis shows the same tendency of the damping rate γ on the magnetic field strength, i. e., for a fixed radial wave length k_r, the larger the ion gyroradius $\rho_i \propto v_{th}/B$ is, the faster the GAM damping rate is. Thus it is confirmed that the FOW effect enhances collisionless damping. It is to be noted, if the FOW effect is neglected ($k_r\rho_i \to 0$ in the formula in Ref.[2]), the damping rate is about $1/10$ of that obtained from our simulations. Therefore, the rapid damping we found in simulations cannot be explained without the FOW effect. Since bounce frequency of trapped particle is much smaller than the GAM frequency $\omega_G \simeq \sqrt{7}v_t h/2R_0$, trapped particles are not so much involved in the resonant damping process. Typical radial excursion of passing particles is about $q\rho_i$, however, as we have shown here, even the small FOW effect $qk_r\rho_i << 1$ brings

substantial enhancement of GAM damping. It also suggests that the FOW effect on GAM is significant for high temperature core region where the gyroradius is large. It explains why the damping rate changes larger on the inner flux surface compared with the outer surface, as shown in Fig. 2.
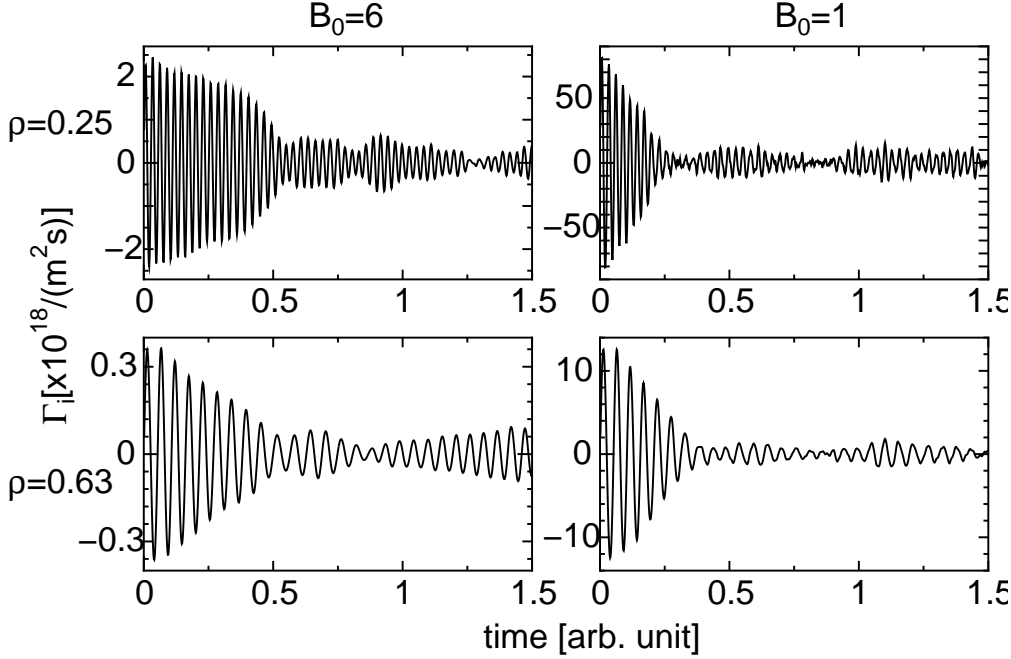

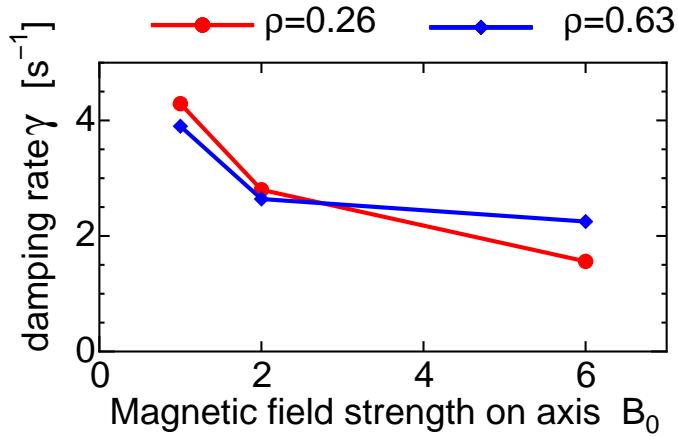*FIG. 1: Time evolution of the ion flux in different magnetic field strength.*

FIG. 2: Dependence of collisionless GAM damping rate on magnetic field strength.

4. Collisionless GAM damping (ii) effect of helical magnetic field

To see the effect of helical magnetic field on GAM, several calculation were carried out. A model Large Helical Device (LHD) configurations are used, with different magnetic axis position $R_{ax} =$3.52, 3.62, and 3.77m. The magnetic field is expressed in Boozer coordinates as $B(\rho, \theta, \zeta) = \sum_{m,n} B_{m,n}(\rho)cos(m\theta - 10n\zeta)$. Note that the current profile was controlled in obtaining MHD equilibrium so that the rotational transform profiles $\iota(\rho)$ become the same among these three configurations. This is because the GAM damping rate also depends on the value of ι, and we intend to see the difference of damping rate when only the Fourier component of the magnetic field $B_{m,n}$ changes.

The LHD configuration with $R_{ax} =3.77$ has the most simple components, in which only three components $(m, n) = (0, 0)$, $(1, 0)$ and $(2, 1)$ are significant. As the magnetic axis shifts toward inward, sideband components such as $(m, n) = (0, -1)$, $(1, 1)$ and $(3, 1)$ arise. The major components of $B_{m,n}$ are shown in Fig. 3. Inwardly shifted configuration is known as an optimized configuration to reduce neoclassical transport. Then it is interesting to see how the behavior of GAM changes in the optimized configuration. On the other hand, we are also interested in investigating which components $B_{m,n}$ are effective to change the behavior of GAM. Therefore, the simulations were done by gradually changing the number of $B_{m,n}$-components used in FORTEC-3D calculation, from only the most significant 3 components to 6, and 12 components, which include higher-(m, n) spectrum.
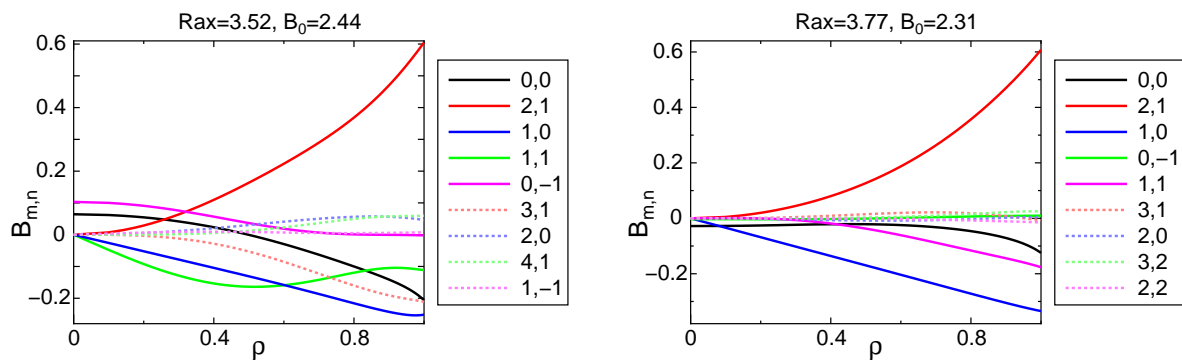

FIG. 3: *Fourier components of the magnetic configuration with $R_{ax} =3.52$ and 3.77m. Here, the line of $(0, 0)$ represents $B_{0,0}(\rho) - B_0$.*

An example of the time evolution of the particle flux and radial electric field are shown in Fig. 4. The GAM oscillation is gradually damping, and finally settled in the ambipolar status $\Gamma_i(\rho) = \Gamma_e(\rho)$. One can see the amplitude of GAM, the frequency, and the damping rate differ according to the major radius. The damping rate is evaluated as in the same way shown in the previous section, and the result is shown in Fig. 5. Generally, the collisionless damping rate γ is much higher in LHD configurations compared with that in a comparable scale tokamak. Consequently, the FOW effect on damping rate is not so significant in helical configurations. Only one helical component $B_{2,1}$ added to axisymmetric tokamak field changes damping rate significantly, as one can see by comparing Fig. 2 and the three-components calculation results in Fig. 5. Concerning to the shift of major axis, the inward shift configuration $R_{ax} =3.52$ shows a remarkable enhancement of γ, especially in the inner flux surface. However, in the calculation where only three Fourier components are used, the relative strength of these components $(m, n) = (0, 0)$, $(1, 0)$ and $(2, 1)$ changes not so much. Therefore, it seems that not only the relative strength of each components, as shown in Sugama and Watanabe's analysis, but also the change of geometry, or the change of the geodesic curvature, affect the GAM damping rate. Moreover, the damping rate changes in the $R_{ax} =3.52$ case largely if as much as 12 components are used in FORTEC-3D. In that case, the relative strength of these higher-(m, n) components are only a few % of the total magnetic field strength, but we found these small components are also effective for the collisionless damping of GAM. Note that in a realistic LHD configuration, the ι value becomes larger and close to or go above unity as the magnetic axis moves inward. Then strong reso-

nant damping of GAM will occur in the inwardly-shifted configuration, though in the present calculation the ι profile is fixed below unity.
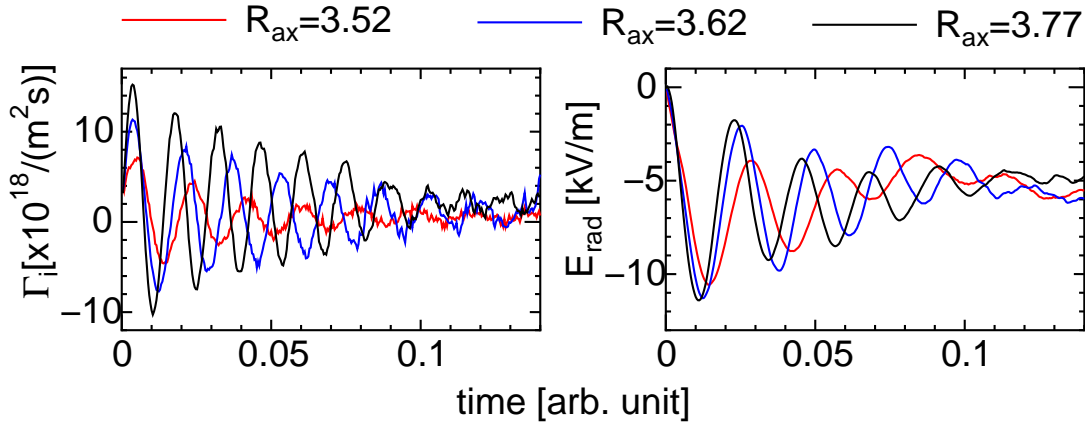

FIG. 4: *Example of GAM oscillation in LHD configuration on $\rho = 0.50$ surface. Here, the most significant 6 components of magnetic field spectrum are used in calculations.*
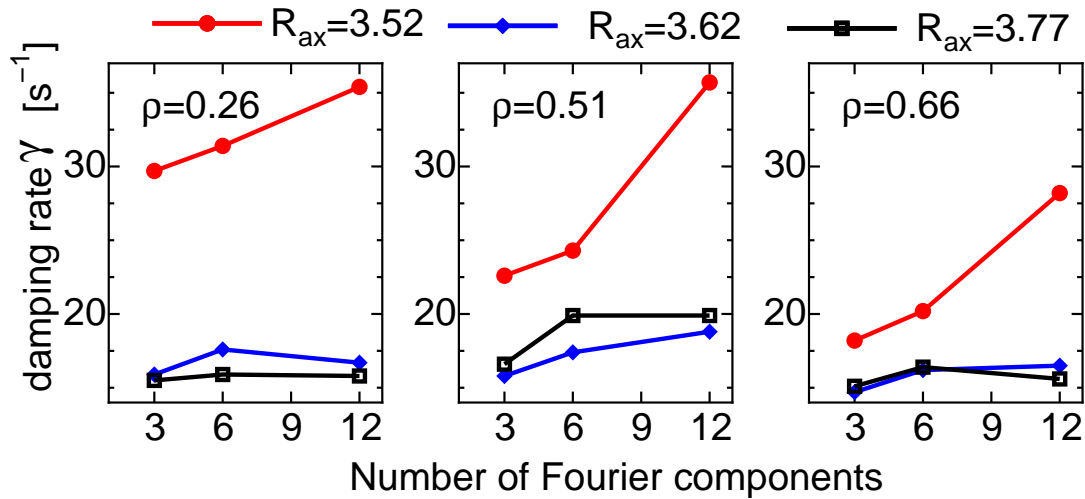

FIG. 5: *Comparison of GAM damping rate in different configuration on three surfaces.*

5. Effect of Collisions on GAM damping

Next, we inspect here the dependency of GAM damping on Coulomb collision. As collisionless damping is too fast in helical systems, we compare the collisional GAM damping in the simple tokamak geometry used in Sec. 3. Simulations were carried out in five different collisionalities, from collisionless limit to plateau regime $\nu_i^* \simeq 2$, where $\nu_i^* = \nu_{ii} q R_0 / \epsilon^{3/2} v_{th}$ is the normalized collisionality. The collisionality is controlled by varying ion density, but the same magnetic field was used in these simulations. Figure 6 shows the time evolution of the ion flux in each collisionality. As the collisionality becomes higher, the beat pattern, which is considered as a non-local effect, disappears. In plateau regime, the wave form becomes a simple exponential damping, as found in Novakovskii's calculation[5] which does not contains any non-local effects. However, as shown in Fig. 7, we cannot find clear dependency of the damping rate γ on collisionality. Several fittings for the result concerning to the dependence on the inverse aspect-ratio ϵ were tested. It is found, as shown in Fig. 8, that the

collisional damping rate seems to have the dependency $\gamma \sim \nu_i/\epsilon$ in plateau to banana-plateau transition regimes $\nu_i^* > \sim 1$. In banana regime, collisionless damping becomes dominant, and γ approaches the collisionless-limit value.
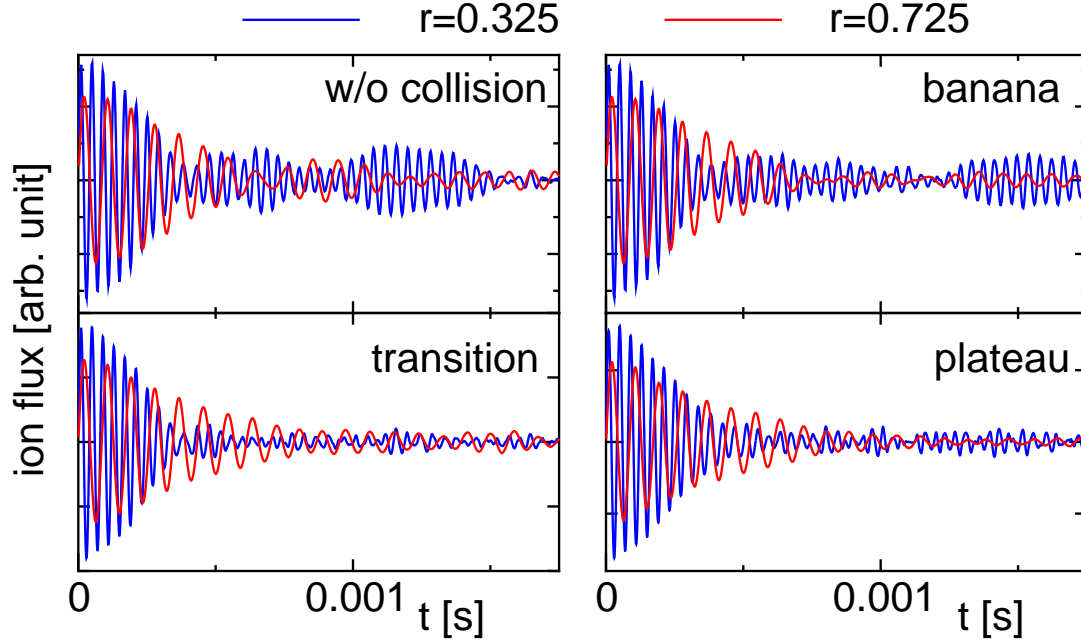

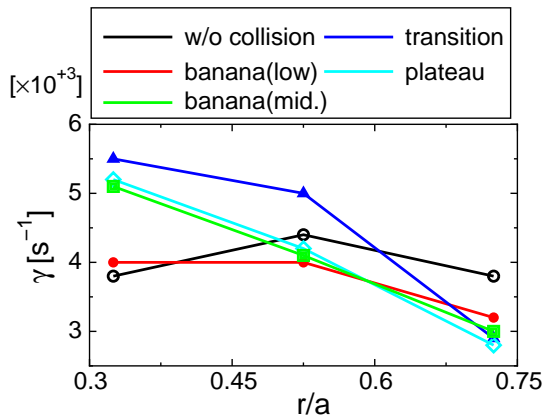FIG. 6: *Time evolution of the ion flux in a tokamak configuration in different collisionality.*

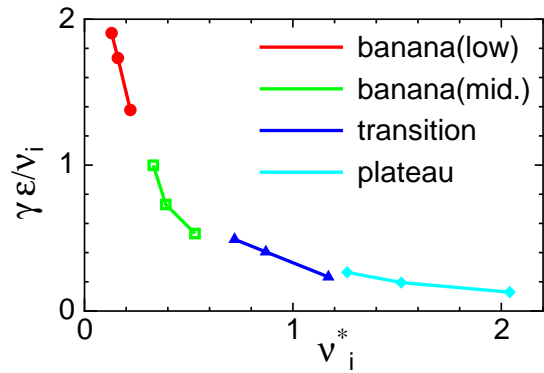FIG. 7: *Dependence of the GAM damping rate γ on three positions in different collisionality.*

FIG. 8: *Dependence of the GAM damping rate on collisionality and inverse aspect-ratio ϵ.*

6. Summary

In the present article, we have shown several simulation results about collisionless and collisional damping of GAM in a drift kinetic model. It was found that the finite-orbit-width effect considerably changes the collisionless damping rate as suggested in Ref.[2]. Further, we found that the inward-shifted LHD configuration has a large collisionless damping rate for GAM. Miyato *et al.*[9] has suggested, in the study of global characteristics of zonal flow by using Landau fluid simulation, that if the oscillatory zonal flow, i. e., GAM damps well, then the residual zonal flow can quench microscopic turbulence. Then it is expected that the

neoclassical optimized LHD configuration would also be desirable for suppressing anomalous transport by zonal flow. However, our simulation model cannot predict the residual zonal flow level. Comprehensive understanding of zonal flow and GAM oscillation, with consideration of non-local and neoclassical effect, would be achieved only by intensive collaboration study between drift kinetic and gyrokinetic studies.

Concerning to the effect of collisions, several existing results for the damping rate dependency on ϵ in Ref.[3]. Among them, Stix's analysis[10] for banana region predicts $\gamma \sim \nu_i/\epsilon$. However, we need to examine more widely in the parameter space to understand the collisional damping effect on GAM, especially in the case both the collisional and collisionless damping are comparable.

Acknowredgement

References

[1] WATARI, T. *et al.*, Phys. Plasmas **12** (2005) 062304.
[2] SUGAMA, H. and WATANABE, T.-H., Phys. Plasmas **13** (2006) 012501.
[3] LEBEDEV, P. N., *et al.*, Phys. Plasmas **3** (1996) 3023.
[4] SATAKE, S. *et al.*, Nucl. Fusion **45**, 1362 (2005).
[5] NOVAKOVSKII, S. V., *et al.*, Phys. Plasmas **4** (1997) 4272.
[6] LIN, Z., *et al.*, Phys. Plasmas **2** (1995) 2975.
[7] WANG, W. X., *et al.*, Plasma Phys. Control. Fusion **41** (1999) 1091.
[8] BEIDLER, C. D. and MAAßBERG, H., Plasma Phys. Control. Fusion **43** (2001) 1131.
[9] MIYATO, N. *et al.*, Phys. Plasmas **11** (2004) 5557.
[10] STIX, T. H., Phys. Fluids **16** (1973) 1260.